24th COBEM - 2017

24th ABCM International Congress of Mechanical Engineering
December 3-8, 2017, Curitiba, PR, Brazil

COBEM-2017-0861
THERMAL MODELING OF CAVITY-RECEIVER FOR CONCENTRATED SOLAR ENERGY

Luma Fonseca do Canto
José R. Simões-Moreira
SISEA – Alternative Energy Systems Lab.
Mechl. Eng. Dept. - Escola Politécnica at University of São Paulo, Brazil
lumacanto@usp.br, jrsimoes@usp.br

Abstract: *Recent worldwide concerns on CO_2 emission and anticipation of fossil fuel decreasing usage have increased the number of research on renewable energy. In Brazil, several agendas were implemented in last years on attempts of diversifying the well-established hydraulic power plants for electricity production and minimizing environmental harmful effects. In this context, the solar energy is highlighted as a promising source since concentrated solar power (CSP) plants already represent a fair amount of total energy produced in developed countries such as USA. and Spain. Therefore, the aim of this work is to analyze the cavity of a CSP system and develop a basic thermal model. Therefore, heat losses in the cavity occurring by re-radiation and convection at the window have been studied, as well as heat losses in the cavity-receiver body. The model was successfully implemented and can be used for various applications.*

Keywords: *Solar energy, cavity-receiver, renewable energy, thermal modeling.*

1. INTRODUCTION

One of the humanity's greatest challenges is to supply the increasing energy demand. Once this issue is solved using a clean and low-cost energy, it would settle other concerns such as pollution, food production, drinking water supply, and so on (Smalley, 2005). Solar energy is largely available in Brazil and furthermore is almost carbon-free (IEA, 2009). But there are some drawbacks: the dispersion and the intermittency. Due to these barriers, it is necessary to collect, concentrate and, if possible, storage the solar energy. In this, the concentrated solar power (CSP) may be an excellent option on the matter.

It is important to know that the Brazilian electrical power grid is largely dominated by hydraulic power, accounting 61,2% of total (ANEEL, 2017), which can be dependent on problems such as drought periods. The second place on power supply is held by fossil fuels (16,6%). The use of CSP is a good answer to diversifying this grid taking into account the welfare of the planet.

The CSP is a system used to generate solar power by concentrating solar thermal energy onto an reflective surface. It works based on direct normal irradiance (DNI), which is highly abundant on the northeast region of Brazil, as show in Fig. 1. Solar thermal energy is not yet economic competitive, but if it relies on well thought incentive programs (Marques, 2015), it can lead to a positive feedback. Lessons can be learned from mistakes and successes of countries where the CSP was successfully added up to the power grid, such as USA. (Fthenakis, *et al.,* 2009), Spain (Martín *et al*., 2015), India (Aruna Kumarankandath, 2015) and Morocco (Frisari and Stadelmann, 2015; Perez *et al.,* 2014).

A CSP system is composed, mainly by a reflecting mirror and a cavity. Figure 2 shows a schematic model in which one can see solar rays being reflected by a parabolic dish mirror, working as concentrator and reflector, to the solar cavity-receiver located at the focal point of the paraboloid. Currently, there are four kinds of CSP technologies: parabolic through, parabolic dish, Fresnel lens, and solar tower. Cavities may be as diversified as it can be modeled and built. A high-flux solar simulator consisting on sky searchlights (Xenon lamps), a paraboloid mirrored surface and a cylindric cavity has been designed and built at SISEA laboratory at University of São Paulo by Rodrigues, *et al.* (2014).

Thus, it is important to understand the cavity-receiver behavior, heat losses involved – which are increased by the high temperatures – and material and geometry effects in order to properly design the right cavity for each application.

Although the main losses mechanisms in the receiver are due to reflection, radiation, conduction and convective heat losses through the cavity aperture, it is necessary to study the magnitude of all kinds of losses.

Harris and Lenz (1985) estimated the heat losses on the CSP system operating from 550ºC to 900ºC as follows: the greatest loss is due to imperfect concentrator surface reflectivity (less than 1%), followed by a vast loss due to radiation spillage around the cavity aperture and re-radiation, relatively expressive loss by convection through the cavity aperture and minimum losses caused by conduction through the walls and shadowing of the concentrator produced by the cavity position.

Figure 1. Direct Normal Irradiation in Brazil (Solargis, 2016)

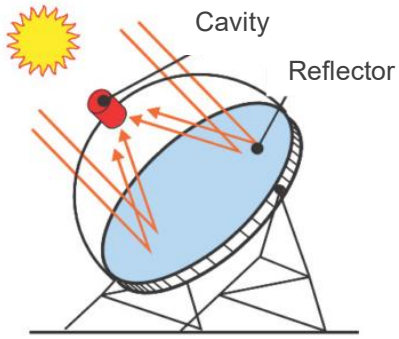

Figure 2. Parabolic dish concentrator diagram. Adapted from (Abbasi-Shavazi et al., 2015)

A 3D numerical modeling has been performed on the effect of various parameters on heat loss of a solar parabolic dish, judging that the cavity inclination is the main source of heat loss on natural convection and cavity cover emissivity on the radiative loss. A study performed by Prakash *et al.* (2009) showed that the inclination is very important when analyzing losses, reaching its maximum loss at 0º inclination and its minimum at a variable angle depending on wind speed. A natural convection heat loss model has been implemented by Samanes *et al.* (2015) and a comparative study of thermal losses on three kinds of receivers for solar dish collector is carried by Sendhil Kumar and Reddy (2008).

An experimental study on the convective losses for several cavity inclination angles and temperatures given a cylindrical cavity was carried by Abbasi-Shavazi *et al.* (2015). Those authors state that it may not be a fine approximation to assume the wall temperature is constant observed its wide and systematic variations. This also justifies the need of analyze the heat losses through the wall.

The influence of receiver geometry on the efficiency of the system is further analyzed by several authors. A numerical 3D model was developed to analyze the thermal losses of a cylindrical solar receiver showing that a cavity whose length spans between 400 and 640mm achieves an optimum thermal efficiency (balance between heat losses and heat transfer areas) given a known set of conditions and proved that the heat losses increase when the aperture diameter increases (Zou *et al.,* 2017). The heat loss dependency of depth of a cylindrical cavity was also numerically studied by Tu *et al.* (2014). Those losses on a semi-spherical cavity were experimentally investigated by Tan *et al.* (2014) and correlated to the Nusselt number. Conclusions on the optimum aperture size and operating temperature are drawn by Steinfeld and Schubnell (1993).

According to Fleming *et al.* (2017), it is important to the cavity designer to know the material limitation on the working temperature, as well as the absorptivity of the material (if effective absorptivity is much larger than the material's, the receiver is assumed to be a blackbody) and its reflectivity.

The main goal of a cavity window is to allow operation of high pressure gases, once the inside of cavity will be isolated from the outside and to minimize losses caused by reflection of radiation entering the cavity and emissions from its inside (O Mande and Miller, 2011). These same authors summarize that a spherical fused silica window correspond to great optical and mechanical manufacturability for a high performance solar cavity. Furthermore, Shuai *et al.* (2011) stated that a plano-convex quartz window can redistribute the radiative flux on a more uniform way than a windowless cavity.

The model implemented in this work investigates radiation, convective and conductive losses throughout the cavity aperture, walls and body as a whole. This study allows determining which parameters may be assorted in order to achieve the best-case scenario. In other words, how to reach the operating temperature for each cavity employment.

The cavity-receiver may be used to generate thermal and electric power using working fluid and thermoelectric modules, with or without thermal storage system (Al-Nimr *et al.*, 2017), hybridized as heat source to organic Rankine cycle (ORC) (Loni *et al.*, 2016) or as thermochemical reactor to produce syngas from methane reforming (Yuan *et al.,* 2017) or hydrogen from metal/oxides pairs (Nigro, Simões-Moreira, 2016) ,biomass gasification (Bellouard *et al*., 2017), among others. This work focus on a reactor cavity.

2. CAVITY MODELING

The cavity-receiver investigated in this article is a cylindrical one as this geometry has been well studied by other authors. It is constituted by a hollow body covered by thermal insulation and an opening aperture at the focus, with a crystal window to guarantee minimum thermal losses. Figure 3 presents side and 3D views of the suggested cavity design.

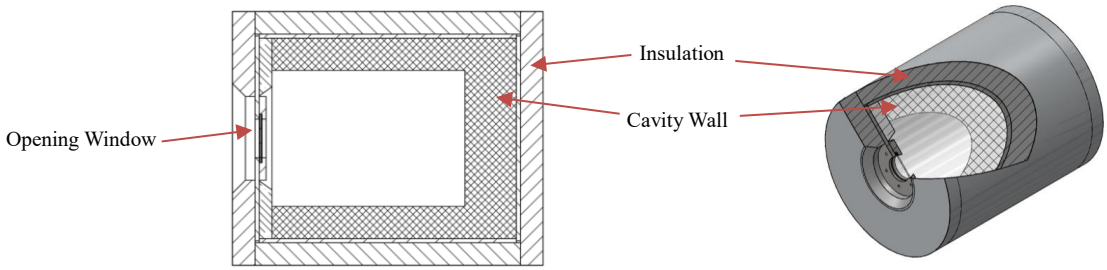

Figure 3. Hollow cylindrical cavity. (a) Side view (b) 3D view

Thermal losses of conduction, convection and radiation are analyzed, as well as the influence of the aperture window size and the heat absorbed by the chemical reaction will be studied. To perform the utmost modeling, it is important to understand all the losses working individually through the window and on the cavity. Figure 4 shows an expanded model, on which of heat fluxes and losses are presented.

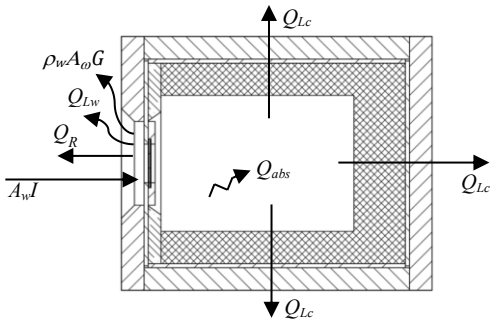

Figure 4. Heat fluxes through the cavity

This way the thermal equilibrium of the cavity is written according to the first law of thermodynamics as given by Eq. (1), which can be rearranged as Eq. (2), being $\tau_{wi}=1-\rho_w$.

$$A_w G=Q_R+\rho_w A_w G + Q_{Lw}+Q_{Lc}+Q_{abs} \quad (1)$$

$$\tau_{wi} A_w G=Q_R+Q_{Lw}+Q_{Lc}+Q_{abs} \quad (2)$$

where:

A_w is the window area [m^2];
G is the sun irradiance [W/m^2];
Q_R is the thermal radiation heat loss of the heat flowing out the window (reirradiation) [W/m^2];
ρ_w is the window reflectivity related to the sun irradiance reflected by the window [-];
τ_{wi} is the window transmissivity related to the thermal radiation entering the cavity [-];
Q_{Lw} is the conduction and convection heat losses through the window [W];
Q_{Lc} is the conduction and convection heat losses through the cavity walls [W];
Q_{abs} is the useful heat absorbed by any chemical reaction occurring inside the cavity [W].

Therefore, the losses mechanisms may be listed as radiation, conduction and convection of the heat flowing out the window, heat reflected by the glass of the opening window and conduction and convection trough cavity walls. The useful heat absorbed by the chemical reaction is the difference between the irradiance on the opening window and the sum of all losses mechanisms.

To help determining these quantities, equivalent electric circuits have been used. Figure 5 represents the radiation circuit and Fig. 6 the conduction and convection circuit.

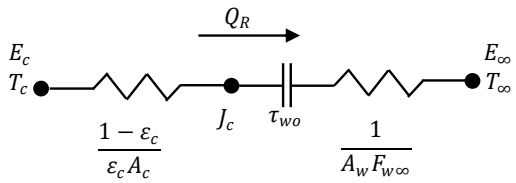

Figure 5. Radiation analogic electric circuit

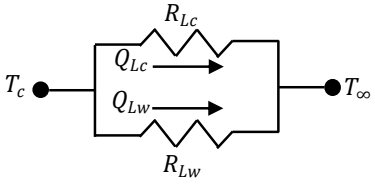

Figure 6. Conduction and convection analogic electric circuit

For the circuits of Fig. 5 and 6, the following quantities are defined:

T_c is the temperature inside the cavity [K];
T_∞ is the surrounding temperature [K];
E_c is the emissive power of the cavity [W/m^2];
E_∞ is the emissive power of the surround [W/m^2];
ε_c is the emissivity of the internal area of the cavity [-];
A_c is the cavity internal area [m^2];
J_c is the cavity radiosity [W/m^2];
$F_{w\infty}$ is the shape factor of the window to the surrounding (=1) [-];
R_{Lc} is the equivalent resistance to conduction and convection through the cavity walls [K/W];
R_{Lw} is the equivalent resistance to conduction and convection through the window [K/W].

Heat losses by radiation, Q_R, conduction and convection through the cavity walls, Q_{Lc}, and window, Q_{Lw}, are written as Eq. (3), (4) and (5), respectively. The useful absorbed heat available for chemical reaction or simple fluid heating is given by Eq. (6).

$$Q_R = \frac{E_c - E_\infty}{R_R} = \frac{\sigma(T_c^4 - T_\infty^4)}{R_R} \tag{3}$$

$$Q_{Lc} = \frac{T_c - T_\infty}{R_{Lc}} \tag{4}$$

$$Q_{Lw} = \frac{T_c - T_\infty}{R_{Lw}} \tag{5}$$

$$Q_{abs} = \mu_{abs} A_w G \tag{6}$$

where:
R_R is the equivalent resistance to radiation [m^2];
σ is the Steffan-Boltzmann constant = 5.67 x 10^{-8} W/m^{2}K^4.
μ_{abs} is the heat fraction absorbed by any chemical reaction inside the cavity from the incident irradiance [-].

Then, substituting these relations in Eq. (1), the equilibrium cavity temperature, T_c, can be rewritten as Eq. (7).

$$T_c^4 + T_c \frac{R_R}{\sigma}\left(\frac{1}{R_{Lw}} + \frac{1}{R_{Lc}}\right) = T_\infty^4 + T_\infty \frac{R_R}{\sigma}\left(\frac{1}{R_{Lw}} + \frac{1}{R_{Lc}}\right) + (\tau_{wI} - \mu_{abs}) A_w G \frac{R_R}{\sigma} \tag{7}$$

Also, the analysis of the absorptivity of the cavity is necessary. The Kirchoff law stablishes that cavity emissivity is equal to the cavity absorptivity ($\alpha_c = \varepsilon_c$), when thermal equilibrium between the cavity and the existing matter inside of it is achieved. Knowing that the equivalent resistance to radiation is given by Eq. (8) and applying the Kirchoff law, the Eq. (9) is attained. Being τ_{wo} the window transmissivity related to the thermal radiation leaving the cavity (dimensionless).

$$R_R = \frac{1}{\tau_{wo}}\left(\frac{1-\varepsilon_c}{\varepsilon_c A_c} + \frac{1}{A_w F_{w\infty}}\right) \tag{8}$$

$$R_R = \frac{1}{A_w}\left[\frac{1}{\tau_{wo}}\left(\frac{1}{F_{w\infty}} + \frac{(1-\alpha_c)}{\alpha_c}\frac{A_w}{A_c}\right)\right] \tag{9}$$

Thus, the radiation heat loss of Eq. (3) is rewritten per unit of area as Eq. (10) and then the effective absorptivity (α_{ef}) of the cavity is determined by Eq. (11).

$$Q_R = \frac{A_w \sigma(T_c^4 - T_\infty^4)}{\left[\frac{1}{\tau_{wo}}\left(\frac{1}{F_{w\infty}} + \frac{(1-\alpha_c)}{\alpha_c}\frac{A_w}{A_c}\right)\right]} \tag{10}$$

$$\alpha_{ef} = \left[\frac{1}{\tau_{wo}}\left(\frac{1}{F_{w\infty}} + \frac{(1-\alpha_c)}{\alpha_c}\frac{A_w}{A_c}\right)\right]^{-1} \tag{11}$$

An important parameter may be introduced is the number of suns (N). This way, the irradiance reaching the cavity opening window is given by $G=NK_{solar}$, where K_{solar} is the sun irradiance equals to 1000W/m^2.

This modeling allows studying the thermal equilibrium and predicting which temperature the cavity achieves for a given number of suns and absorption rate. Also, a study on cavity geometry has been carried. All analyses are made considering ambient temperature is at 298K.

3. RESULTS AND DISCUSSION

First, the goal has been to analyze the effective absorptivity of the cavity on applying Eq. (11), on which the form factor and window transmissivity have been considered equal to one. Figure 7 shows the relation between the window area and internal cavity area ratio (A_w/A_c) and the effective absorptivity for several cavity absorptivities, α_c.

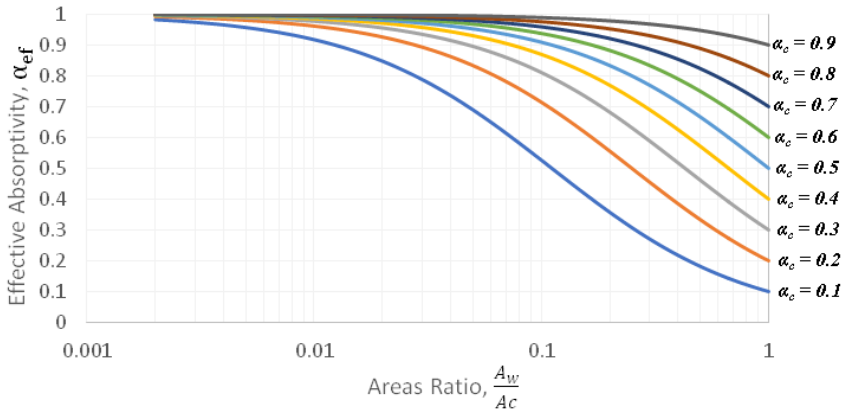

Figure 7. Effective absorptivity, α_{ef}, as a function of areas ratio, A_w/A_c

The results attained in Fig. 7 convey that the smaller the area ratio, the closer the cavity absorptivity is to the black body effectivity, i.e., α_{ef} =1 no matter the material construction and the finishing of the cavity inner wall and the corresponding absorptivity (α_c).

Considering that the cavity is thermally well insulated and the window is made of double glass type, the losses by conduction and convection both through the walls and through the aperture have been considered negligible. This way, the absorption rate is represented by Eq. (12).

$$\mu_{abs}=\frac{G-\alpha_{ef}\sigma(T_c^4-T_\infty^4)}{G} \tag{12}$$

As stated previously, $G=NK_{solar}$. So, the equilibrium temperature of the cavity can be written as Eq. (13).

$$T_c=\sqrt[4]{T_\infty^4+\frac{(1-\mu_{abs})NK_{solar}}{\alpha_{ef}\sigma}} \tag{13}$$

Besides, if the cavity aperture is much smaller than the cavity area, the effective absorptivity is equal to 1 and the relation between equilibrium temperature and absorption ratio for a given number of the suns is presented in Fig. 8. When no heat is absorbed by the chemical reaction, there are no losses on the cavity and the adiabatic temperature is attained, that means it is the maximum temperature the cavity can reach at the thermal equilibrium. If all heat is absorbed by the chemical reaction, the cavity temperature is equal to the ambient temperature, no matter the number of suns.

The adiabatic cavity temperature is achieved for $\mu_{abs}=0$, then it can be written as Eq. (14).

$$T_c=\sqrt[4]{T_\infty^4+\frac{NK_{solar}}{\alpha_{ef}\sigma}} \tag{14}$$

Once the number of suns and the temperature needed for the chemical reaction are known, the rate of heat absorption needed for the chemical reaction can be determined. For example, if the number of suns achieved by the apparatus is 1500

and the temperature needed for the reaction is 1500K, it is possible to know that the heat absorption rate is 80% of the income irradiation, as given by Eq. (6).

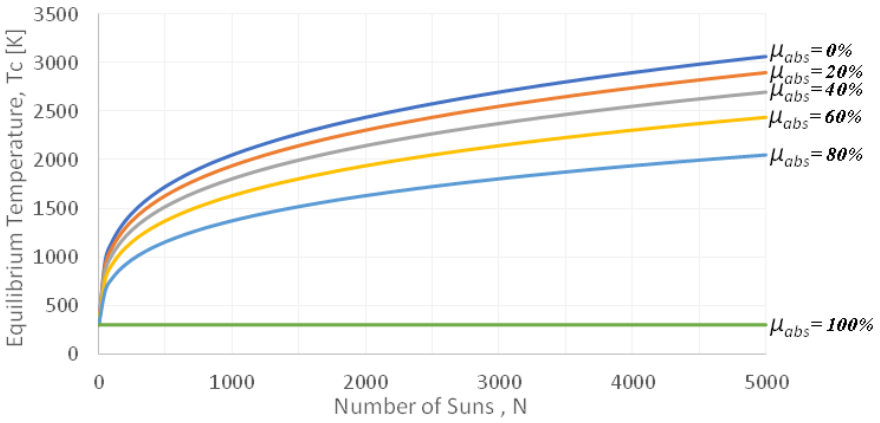

Figure 8. Equilibrium Temperature, T_c, as a Function of the Number of Suns, N

From this information, the necessary flux of mass of the reactant can be determined by Eq. (15).

$$\dot{m}=\frac{\mu_{abs}G}{\Delta h} \tag{15}$$

where:

$\dot{m}$ is the flux mass of the reactant or working fluid [kg/s];

Δh is the specific enthalpy of the reaction or simple heating [kJ/kg].

Thus, the model implemented on this work allows to study the losses mechanisms operating in the cavity-receiver, to deduct its geometry, its absorption rate and the mass flux of the reactant used on the chemical reaction for which the cavity-receiver has been designed.

4. APLICATIONS

Two cases have been studied in order to better comprehend the analysis developed on this paper. The vaporization of water and heating of a downtherm fluid have been eximined, considering the cavity a black body (apperture is much smaller than the cavity inner area).

For both cases, first it has been set the desired temperatures (388K 488K and 628K, chosen based on the available downtherm fluid data) and the corresponding number of suns has been calculeted by rearreging Eq. (13) as Eq. (16), knowing that the constant K_{solar} is equal to 1000W/m^2.

$$N=\frac{T_c^4-T_\infty^4}{1000(1-\mu_{abs})} \tag{16}$$

This way, the number of suns required increase along with the equilibrium temperature powered to four and with the increase on the absorption rate. The results are drawn in Fig. 9, which shows that proportion. It can be confirmed in the image previously arranged in the Fig. 8.

Then, the Eq. (15) has been applied to determine the flux of mass needed to reach the suitable equilibrium temperature and absorption rate. Though, it is important to notice that for each temperature and absorption rate desired, a number of suns has been calculated. It means that when applying Eq. (15), the quantity G (equals to the product NK_{solar}) introduced varies according to the temperature and absorption rate expected to attain.

Thus, once the variation of enthalpy depends on the variation of temperature and K_{solar} is a constant, it can be stated that the flux of mass is a function of the three correlated variables: the number of suns, the absorption rate and the variation of temperature.

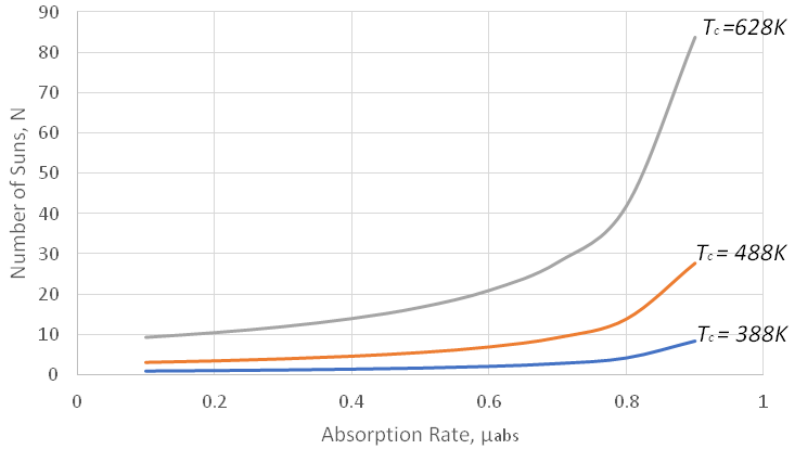

Figure 9. Number of suns, N, as a function of absorption rate, μ_{abs}, to attain desired equilibrium temperatures

4.1 Production of Steam

In order to analyze the mass flux of water required to attain steam at a given temperature, the enthalpy increase for heating in Eq. (15) has been defined as the variation between the enthalpy given at the equilibrium temperature of the cavity and the temperature the water (steam) enters the cavity (set at 298K). Table 1 shows those enthalpies.

Table 1. Enthalpy of Heating for Steam at 1atm.

Equilibrium Temperature [K]	Enthalpy of Heating, Δh [kJ/kg]
388	2601
488	2800
628	2791

Figure 10 represents the results. The flux of water mass increases greatly with the absorption rate and temperature, reaching 27kg/s at 628K for 90% of absorption, versus 0.33kg/s for 10% of absorption at the same temperature. At 388K, 2.9kg/s are necessary for a rate of absorption of 90% and 0.04kg/s for a rate of 10%. A careful analysis must be carried out on interpreting these figures since the number of suns to achieve certain temperature is also a variable parameter as shown in Figure 9. For instance, if a given number of suns is established and a given absorption ratio, less amount of vapor at higher temperature is produced.

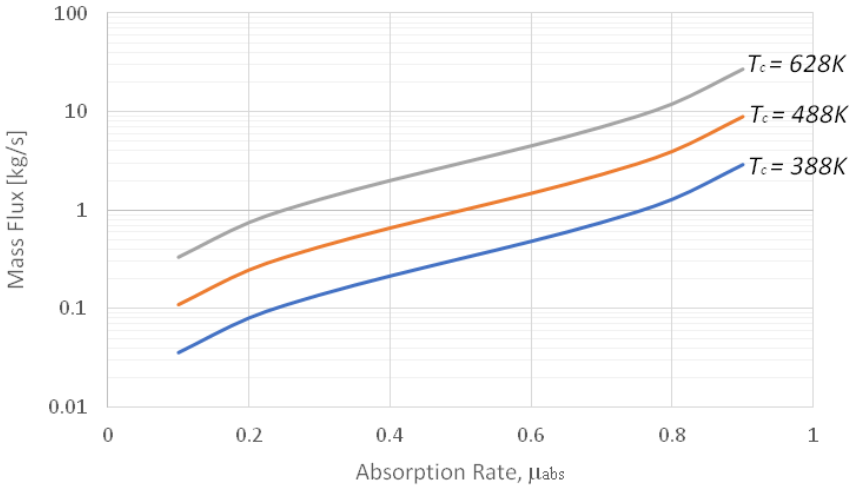

Figure 10. Mass flux of water, $\dot{m}$, as a function of absorption rate, μ_{abs}, at the desired steam saturated temperature

The mass flux varies with the inverse of the variation of enthalpy, which increases with the increment on the temperature as can be seen in Table 1. Although it is important to notice that the mass flux is also a function powered to

fourth of the temperature. This way, the raise of temperature impacts more significantly the mass flux than the difference on the enthalpy of heating, leading to a gain on mass flux with the increase of the temperature.

4.2 Heating of Dowtherm Fluid

Dowtherm Fluid is a mixture of eutectic compounds, mostly used to indirect heat transfer. The Dowtherm G has been chosen for its stability at low pressure and good performance in liquid phase heat transfer systems. Its recommended use temperature range is between 267K and 633K.

Using the data provided by the manufacturer (Dow, 2017), the enthalpy of heating for the chosen Dowtherm fluid is given by Eq. (17), where T_c is the equilibrium temperature given in Kelvin, and considering the fluid initial temperature is at 298K. Table 2 represents the results to attain the desired temperatures.

$$h = 0.0035\frac{T_c^2}{2} + 0.5213T_c - 310.7544 \tag{17}$$

Table 2. Enthalpies of Heating for Dowtherm G

Equilibrium Temperature [K]	Enthalpy of Heating, Δh [kJ/kg]
388	154.96
488	360.39
628	706.79

As can be seen from comparing Table 1 and 2, the enthalpy of heating of the dowtherm fluid is much smaller than the water one, and since the working temperatures are the same for both cases, it leads to greater mass fluxes as shown in Fig. 11. The same observation regarding the amount of heating oil is valid as the one remarked for steam production as stated above concerning the number of suns and the absorption amount.

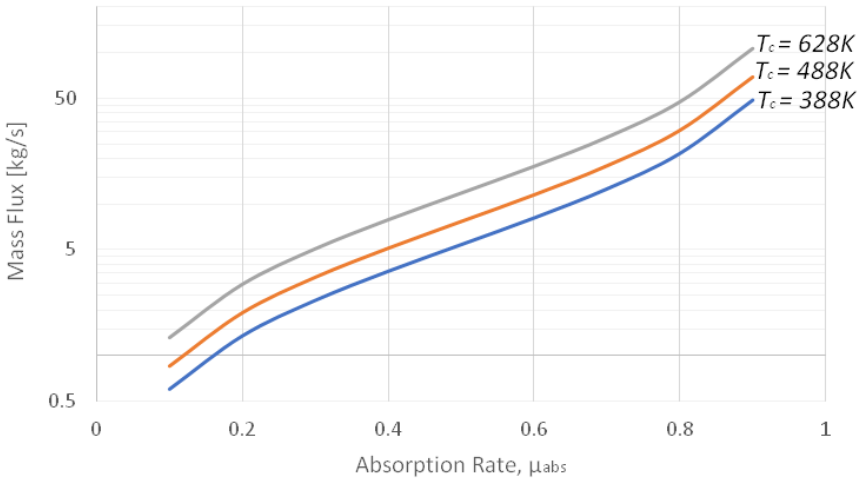

Figure 11. Mass flux of Dowtherm G, $\dot{m}$, as a function of absorption rate, μ_{abs}, at the desired steam saturated temperature

This way, when the cavity reactor goal is to reach high temperatures in order to perform indirect heat flux, it may be interesting to use steam rather than a Downterm fluid, since a much smaller quantity of the first is needed than the last. Also, water is cheaper and widely accessible. On the other hand, the Dowtherm fluid has advantages like not corroding metal and common alloys.

5. CONCLUSIONS

Destructive effects of CO_2 emission increased the concern on the matter of an alternative energy source on way to replace or complement the use of fossil fuels. One of the most promising renewable energy sources is the solar energy, which can be used to generate electricity or as heat source for distinct applications.

The analysis of the losses occurring on the cavity-receiver of the CSP system indicates if the apparatus is really efficient and lead to a correct design fitting specific application. The knowledge of its imperfections permits the minimization of its losses mechanisms and boosts its performance.

The model developed on this article can be used to several processes, showing that on assigning good relation between areas of cavity and cavity aperture, the cavity-receiver works as a black body. Also, it leads to a detailed analysis of the chemical reaction absorption rate and the necessary reactant mass flux.

Finally, despite the valuable information attained, it is still required to carry out experimental studies and to add new details to the research. As suggestions for future work, study on other cavity geometries may be pertinent. Additionally, it would be interesting to carry these analyses to a determined application.

6. ACKNOWLEDGMENTS

We gratefully acknowledge support of the RCGI – Research Centre for Gas Innovation, hosted by the University of São Paulo (USP) and sponsored by FAPESP – São Paulo Research Foundation (2014/50279-4) and Shell Brasil.

The first author thanks CAPES for personal support.

7. REFERENCES

Abbasi-Shavazi, E., G. O. Hughes *et al.,* 'Investigation of Heat Loss from a Solar Cavity Receiver', *Energy Procedia*, 69 (2015), 269–78

ANEEL, 'Capacidade de Geração Do Brasil', 2017, pp. 7–8 <http://www2.aneel.gov.br/aplicacoes/capacidadebrasil/capacidadebrasil.cfm> Accessed in 1 July 2017.

Al-Nimr, M. A., Bourhan, M. T., *et al.,* 'A Hybrid Concentrated Solar Thermal Collector / Thermo-Electric Generation System', *Energy*, 134 (2017), 1001–12

Bellouard, Q., Stéphane A., *et al.,* 'Solar Thermochemical Gasification of Wood Biomass for Syngas Production in a High-Temperature Continuously-Fed Tubular Reactor', *International Journal of Hydrogen Energy*, 42 (2017), 13486–97

Dow, 'Technical Data Sheet: Dowtherm G' <http://www.dow.com/heattrans/products/synthetic/dowtherm.htm> Acessed 05 October 2017.

Fleming, A., Charles F. *et al,* 'A General Method to Analyze the Thermal Performance of Multi-Cavity Concentrating Solar Power Receivers', *Solar Energy*, 150 (2017), 608–18

Fthenakis, Vasilis, James E. Mason, and Ken Zweibel, 'The Technical, Geographical, and Economic Feasibility for Solar Energy to Supply the Energy Needs of the US', *Energy Policy*, 37 (2009), 387–99

Gianleo, F. and Stadelmann, M., 'De-Risking Concentrated Solar Power in Emerging Markets : The Role of Policies and International Fi Nance Institutions', *Energy Policy*, 82 (2015), 12–22

Harris, J. A., and Lenz, T.G., 'Thermal Performance of Solar Concentrator/cavity Receiver Systems', *Solar Energy*, 34 (1985), 135–42 <http://dx.doi.org/10.1016/0038-092X(85)90170-7>

IEA, 'Renewable Energy Essentials: Concentrating Solar Thermal Power', 2009, pp. 1–4 <http://www.iea.org/papers/2009/CSP_Brochure.pdf>

Kumarankandath, A. and Goswami, N. 'The State of Concentrated Solar Power in India: A Roadmap to Developing Solar Thermal Technologies in India', ed. by Archana Shankar, *Centre for Science and Evironment* (New Delhi: Centre for Science and Evironment, 2015)

Kumar, N.S., and Reddy, K.S., 'Comparison of Receivers for Solar Dish Collector System', *Energy Conversion and Management*, 49 (2008), 812–19

Loni, R., Kasaeian, A.B., *et al.* 'Performance Study of a Solar-Assisted Organic Rankine Cycle Using a DishMounted Open-Cavity Tubular Solar Receiver', *Applied Thermal Engineering*, 18 (2016), 1298–1309

Mande, O. K., and Miller, F., 'Window Design for a Small Particle Solar Receiver', *Iecec 2011*, 2011

Marques, R.S., 'Energia Solar No Brasil: Dos Incentivos Aos Desafios', 2015

Martín, H., Jordi D.L.H., *et al.*, 'Promotion of Concentrating Solar Thermal Power (CSP) in Spain: Performance Analysis of the Period 1998-2013', *Renewable and Sustainable Energy Reviews*, 50 (2015), 1052–68

Nigro, L. G. and Simões-Moreira, J. R., 'Cavity Receiver Conception for Chemical Reactors Using Solar Energy'. 16th Brazilian Congress of Thermal Sciences and Engineering, Vitória, 2016.

Perez, I., Lopez, A., *et al.*, 'National Incentive Programs for CSP – Lessons Learned', *Energy Procedia*, 49 (2014), 1869–78

Prakash, M., Kedare, S.B., *et al.*'Investigations on Heat Losses from a Solar Cavity Receiver', *Solar Energy*, 83 (2009), 157–70

Rodrigues, J. D. R. H., Ribas, V. E., *et al.,* 'Design and Building of a Compact Solar Simulator with Radiation Concentration'. 15th Brazilian Congress of Thermal Sciences and Engineering, Belém, 2014.

Samanes, J., García-Barberena, J. *et al.,* 'Modeling Solar Cavity Receivers: A Review and Comparison of Natural Convection Heat Loss Correlations', *Energy Procedia*, 69 (2015), 543–52

Smalley, R. E., 'Future Global Energy Prosperity: The Terawatt Challenge', *MRS Bulletin*, 30 (2005), 412–17

Solargis, ‘Solar Resource Maps for Brazil’, 2016 <http://solargis.com/products/maps-and-gis-data/free/download/brazil> [accessed 1 April 2017]

Steinfeld, A., and M. Schubnell, ‘Optimum Aperture Size and Operating Temperature of a Solar Cavity-Receiver’, *Solar Energy*, 50 (1993), 19–25

Tan, Y., Zhao, L., *et al.,* ‘Experimental Investigation on Heat Loss of Semi-Spherical Cavity Receiver’, *Energy Conversion and Management*, 87 (2014), 576–83

Tu, N., Jinjia W., *et al.*, ‘Numerical Study on Thermal Performance of a Solar Cavity Receiver with Different Depths’, *Applied Thermal Engineering*, 72 (2014), 20–28

Yong, S., Fu-Qiang W., *et al.,* ‘Radiative Properties of a Solar Cavity Receiver/reactor with Quartz Window’, *International Journal of Hydrogen Energy*, 36 (2011), 12148–58

Yuan, Q., Ding, J., *et al.* ‘Transient Thermochemical Storage Performance of Methane Reforming in Semi-Cavity Reactor Heated by Solar Dish System’, *Energy Procedia*, 105 (2017), 398–405

Zou, C., Zhang, Y., *et al.,* ‘Effects of Geometric Parameters on Thermal Performance for a Cylindrical Solar Receiver Using a 3D Numerical Model’, *Energy Conversion and Management*, 149 (2017), 293–302

8. RESPONSIBILITY NOTICE

The authors are the only responsible for the printed material included in this paper.